Journal of Materials Chemistry B

ROYAL SOCIETY OF CHEMISTRY

PAPER

View Article Online
View Journal | View Issue

Cite this: J. Mater. Chem. B, 2024, 12, 10068

Self-assembled thin films as alternative surface textures in assistive aids with users who are blind†

Zachary Swain, ‡[a] Maryanne Derkaloustian,‡[a] Kayla A. Hepler, [a] Abigail Nolin,[a] Vidhika S. Damani,[a] Pushpita Bhattacharyya, [bc] Tulaja Shrestha,[d] Jared Medina,[be] Laure V. Kayser [ad] and Charles B. Dhong *[af]

Received 26th July 2024,
Accepted 5th September 2024

DOI: 10.1039/d4tb01646g

rsc.li/materials-b

Current tactile graphics primarily render tactile information for blind users through physical features, such as raised bumps or lines. However, the variety of distinctive physical features that can be created is effectively saturated, and alternatives to these physical features are not currently available for static tactile aids. Here, we explored the use of chemical modification through self-assembled thin films to generate distinctive textures in tactile aids. We used two silane precursors, *n*-butylaminopropyltrimethoxysilane and *n*-pentyltrichlorosilane, to coat playing card surfaces and investigated their efficacy as a tactile coating. We verified the surface coating process and examined their durability to repeated use by traditional materials characterization and custom mesoscale friction testing. Finally, we asked participants who were both congenitally blind and braille-literate to sort the cards based on touch. We found that participants were able to identify the correct coated card with 82% accuracy, which was significantly above chance, and two participants achieved 100% accuracy. This success with study participants demonstrates that surface coatings and surface modifications might augment or complement physical textures in next-generation tactile aids.

Introduction

For people who are severely visually impaired or blind, touch serves as a critical means to obtain spatial data through accessible tactile aids and graphics.[1] Traditionally, tactile graphics have relied on mechanical textures, like raised bumps, lines, or other physical structures to generate tactile stimuli.[2–4] However, current tactile graphics are not as information-dense as visual graphics.[5] This is partly because the maximum number of distinctive physical textures that are simultaneously interpretable is five,[6] after which, additional variety in physical labels and textures can overwhelm the user.[7] The difference of information density between visual cues and tactile aids contributes to the discrepancies in access, independence, experiences, education, and gainful employment that exist for people who are blind.[8–10]

When exploring a tactile aid, tactile stimuli originate from the friction and adhesion forces generated at the finger-object interface.[11,12] To modulate friction, tactile aids traditionally use physical features like bumps or lines. However, friction can also be modified by surface chemistry.[13] Here, we explored the use of different surface coatings to generate tactile stimuli as an alternative to physical features. We used silane surface coatings to mark the color of playing cards and evaluated the coatings' ability to generate identifiable surface textures on realistic, perceptibly rough surfaces (overview in Fig. 1). Participants who were both congenitally blind and braille-literate were provided playing cards with different silane coatings applied to the black-suited and red-suited cards, and were tasked to identify which was the black card. Participants were able to successfully identify these coated cards, thus establishing that

[a] Department of Materials Science and Engineering, University of Delaware, Newark, DE, USA. E-mail: cdhong@udel.edu
[b] Department of Psychological & Brain Sciences, University of Delaware, Newark, DE, USA
[c] Smith-Kettlewell Eye Research Institute, San Francisco, CA, USA
[d] Department of Chemistry and Biochemistry, University of Delaware, Newark, DE, USA
[e] Department of Psychology, Emory University, Atlanta, GA, USA
[f] Department of Biomedical Engineering, University of Delaware, Newark, DE, USA

† Electronic supplementary information (ESI) available. See DOI: https://doi.org/10.1039/d4tb01646g

‡ These authors made equal contributions to this work.

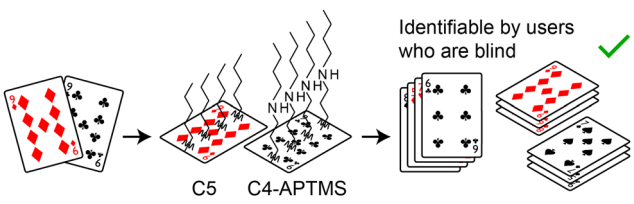

Fig. 1 Playing cards were coated with two different silane precursors, *n*-pentyltrichlorosilane (C5) and *n*-butylaminopropyltrimethoxysilane (C4-APTMS). Participants who were blind and braille-literate successfully identified the coated cards by touch alone.

surface chemistry modification can provide sufficiently salient tactile cues against a physically rough background in assistive aids.

Background

Over four million people are severely visually impaired or blind in the United States, with the prevalence expected to increase to nine million by 2050.[14] People who have limited vision depend on tactile display of information as an alternative to visual graphics in obtaining spatial data and other non-textual information.[15] Tactile graphics convert visual cues into a physical diagram with elements designed to be interpreted by touch,[16] and traditionally convey information through raised bumps, lines, shapes, and braille notation. This tactile information is gathered by fine touch when a finger encounters the mechanical textures present on the surface.[17–20] These physical features provide abrupt changes in adhesion and friction which give rise to distinct tactile percepts.[11,21]

While tactile aids are widely used, a critical limitation is information density.[22] Simply increasing the amount of physical shapes in a given area can often lead to "tactile clutter," complicating interpretation of the content.[7] This hinders complexity and throughput of tactile information as compared to visual graphics. Indeed, current rates of information transmission by tactile cues are much worse than visual all-at-once information gathering and context.[4] This fundamental discrepancy in quality between tactile and visual information presents an accessibility issue for people who are visually impaired or blind.[23]

Individuals who are visually impaired or blind may experience increased tactile acuity from greater reliance on their sense of touch,[24] however, touch provides less spatial resolution than vision, owing to the inherent low-pass filtering of cutaneous processing.[25] Coupled with a substantially more restrictive field of view, detail and spatial context are more difficultly conveyed by touch.[4] These factors both contribute to a significantly decreased bandwidth of information gathering and processing, as compared to visual cues. Lederman *et al.* showed that certain material properties are both discriminable by touch and processed in parallel with shaped physical discontinuities on a surface.[26] Furthermore, the use of chemical features alone is demonstrated to give rise to distinct tactile percepts obtained during touch.[11,27,28] As chemical features were first demonstrated to be discriminable on perceptibly smooth surfaces to eliminate any physical contribution,[27] it is important to next determine whether these features are discriminable on perceptibly rough surfaces which may be used in application of this finding.

Recent advances in materials science or engineering approaches have significantly improved functionality in modern tactile displays,[18] but have not yet overcome the fundamental limitation of tactile clutter. Most recent progress includes powered, dynamic devices as a new form of tactile aid. Refreshable braille displays, or modern electroactive and stimuli responsive polymers, use electromagnetics or electroactive polymers to drive a physical pin up or down.[29] Ren *et al.* developed an actuator using an electrostrictive terpolymer that provides better performance than conventional piezoceramics.[30] Frediani *et al.* leveraged advancements in dielectric elastomers to prototype a braille cell for refreshable, thin displays.[31] Torras *et al.* have utilized composites of carbon nanotubes in a liquid crystal elastomer matrix to create wireless opto-mechanical actuators for tactile displays through thermomechanical actuation.[32] In addition to mechanical actuation, haptic devices, not necessarily implemented as tactile aids, have resulted in a variety of tactile actuation, like electrical, vibrational, and pneumatic.[33] However, Race *et al.* underscore that these technologies pose a prohibitive expense and lack the resolution to recreate spatial data as compared to even current static tactile graphics. Likewise, conventional technologies like piezoceramic bimorph actuators are often too costly and too bulky for widespread adoption.[29] One of the most limiting factors for information density is that these dynamic devices do not provide a fundamental difference in the number of categories displayed than either their conventional form or a traditional static tactile graphic, they are just refreshable.

As an alternative to generating tactile stimuli by bulk physical features, we instead investigated how we might modify the stimuli received from a tactile aid by controlling friction through surface chemistry. From a mechanical perspective, fine touch and tactile sensations originate from the frictional and adhesive forces between the finger and object interface.[11] In applications outside of human touch, friction is well-known to be modified by surface chemistry.[13] A material surface may be considered perceptibly rough when its surface features are greater than ~13 nm, as reported by Skedung *et al.*[34] Prior work has established that molecular-scale effects on perceptibly smooth surfaces, *i.e.* with no surface features above this size limit, are known to influence mesoscale adhesion and friction in fine touch.[11,27,28,35,36] In particular, work by Nolin *et al.* showed that silane coatings can provide distinctive tactile feedback on pristine, perceptibly smooth silicon wafers based on their surface chemistry.[27] When investigating the use of *n*-butylaminopropyltrimethoxysilane (C4-APTMS) and *n*-pentyltrichlorosilane (C5), they found that the C4-APTMS coating maintained similar physical properties as compared to the C5 coating, despite the effect of the amine functional group on the coating's ordering and surface energy. This ordering transition has been well-established in nanoscale atomic force microscopy (AFM) to change friction.[37,38] This prior work establishes that surface chemistry is able to generate discriminable tactile perceptions on pristine, perceptibly smooth surfaces strictly below a ~13 nm physical roughness limit. It also suggests silane coatings as well-controlled pilot materials for tactile discriminability studies. However, prior works leave unanswered whether surfaces that do contain physical roughness, which is characteristic of everyday objects, can be identified by surface chemistry. This open question will be explored in this work to narrow the existing knowledge gap in the literature for effective translation of modern tactile research.

Determining whether two materials will feel different from their chemical structure alone is not yet possible. This difficulty

arises from complication in modeling friction, which is a dynamic process, and the unsuitability of organizing materials by their friction coefficient, which is widely used as a material property despite being a dynamic property.[12,39–41] Works from Lio *et al.* and Barrena *et al.* have offered connections from differences in the bend and tilt of chains, as produced by molecular ordering and packing density, to alterations in friction at the surface.[35,36] They find these molecular-scale effects to influence the material's relative efficiency to store or dissipate the energy introduced by frictional contact. Finally, material properties are also known to be simultaneously processed by fine touch across fingers in parallel with the physical features present on a surface,[26] though no predictive model yet exists. Together, the prior work suggests a possible additional mode of materials design to that of purely physically featured tactile aids. However, investigation of surface chemistry modification as a method to deliver distinct tactile cues as a functional accessibility aid has not yet been explored.

Here, we investigated whether the effects of surface chemistry on friction and adhesion can be leveraged over perceptibly rough surfaces representative of everyday objects to provide distinct tactile cues in order to identify surfaces by touch. To do this, we used silane surface coatings to establish that surface modification can help accessibly interpret information from a functional tactile aid. Given our prior work on pristine, perceptibly smooth surfaces, we used playing cards to represent commonly recognizable everyday objects that can be explored by participants in a manner that reflects everyday usage, allowing us to effectively assess the coatings' utility in application. Unlike silicon wafers, everyday objects have perceptible surface roughness which may or may not obscure differences in touch from surface chemistry, leaving a gap for effective translation of fundamental tactile research to modern accessibility aids, as addressed in this work.

Experimental methods and rationale

Materials system

Silanes were chosen as materials here given that they are commercially available and are comparatively rapid and consistent to coat samples in the numbers needed for human testing. Upon vapor-phase deposition, silanes can form monolayers on surfaces.[40,41] In silanes, the comparatively constant "head" group forms a covalent bond to the surface and the "tail" portion of the silane consists of the desired functional group. This process allows for well-controlled monolayers to form on pristine surfaces, although Oyola-Reynoso *et al.* suggest that a step-growth polymerization of particles can occur over regions of the surface with adsorbed water present in cellulose-based substrates.[42] While important to control for uniformly flat surfaces, the presence of discrete polymerized regions across the surface coating is less of a concern here, as our goals are to use rapid fabrication methods to generate distinctive tactile feedback of everyday surfaces, *i.e.*, surfaces that are already perceptibly rough. As such, vapor-phase deposition of silane precursors was utilized in this work as a scalable coating method, with note and characterization of potential polymerized aggregate regions relative to the limit of human tactile perception ($\sim$13 nm).[34] Here, *n*-butylaminopropyltrimethoxysilane (C4-APTMS) and *n*-pentyltrichlorosilane (C5) were chosen as candidate materials for vapor-phase deposition. The amine functional groups in the C4-APTMS coating increase its surface energy as well as intermolecular interactions by hydrogen bonding to produce a more ordered surface coating than alkylsilanes.[43] This ordering of C4-APTMS provides less modes of energy dissipation, which leads to a reduction in friction,[35] despite maintaining similar physical properties.[27]

Three types of playing cards were first purchased as trial substrates to consider for this study: MaxiAids braille playing cards, VSONE plastic braille playing cards, and Maverick jumbo index playing cards. The Maverick jumbo index playing cards were most consistent in forming surface coatings out of the three brands for vapor deposition of the silane and were selected for use throughout this study. A mechanistic or chemical origin for the improved performance of the Maverick cards is not possible due to proprietary formulation used, but it is likely related to the availability of reactive sites on the card surface after UV-ozone (UV-O_3) treatment for the silanization process. Only numeric cards were used in order to control for potential effects of extensive and varying pigmentation across the surface of face cards.

Sample preparation

The two silanes used in this study were purchased from Gelest at 95–100% purity and were used as-received. The playing cards (Maverick, United States Playing Card Company) were prepared by first subjecting them to UV-O_3 treatment for 15 minutes (PSD Series Digital UV Ozone System at 185 nm and 254 nm, Novascan). The cards were then transferred into vacuum desiccators and at least 50 μL of the respective silane (C4-APTMS for black-suited cards, and C5 for red-suited cards) deposited on a glass microscope slide. Separate desiccators were used for each silane to avoid material cross-contamination. Desiccators were then held under vacuum for 4 hours at room temperature before removing the samples.

Friction characterization and mock finger fabrication

We used a mechanical testing system similar to that first established by Carpenter *et al.*[11,12,27,28] to simulate and record macroscopic frictional forces encountered when a finger slides across the card surface. Although surfaces are commonly characterized through atomic force microscopy, human fingers are an example of mesoscale sliding and have added influence from the elasticity of the finger. In our setup, a polydimethylsiloxane (PDMS) mock finger is slid to generate frictional forces while in contact with the surface. Although the human finger appears rounded, in a sliding mode, the human finger is nearly constant in contact area even at very low pressures, as evidenced by comparatively constant-width residues in real humans, which is why a rectangular geometry was chosen to

reflect a load-independent apparent contact area, as we have done previously.[12,43,44] To fabricate the mock finger, PDMS (Dow Sylgard 184) was prepared in a 30 : 1 base to crosslinker ratio, which has an elastic modulus of ~100 kPa to match the elastic modulus of a human finger. The liquid mixture was then molded into a 5 cm × 1 cm × 1 cm rectangular prism surrounding a 3D-printed acrylic "bone" to approximate the multilayer contributions of the soft tissue and the distal phalange. The mock finger is slid at several combinations of applied mass (M = 0–100 g, added to the deadweight of the finger) and velocity (v = 5–45 mm s^{-1}) to mimic friction experienced during human exploration. Detailed selection of mock finger geometry and properties as a model of the human finger and contact geometry was justified in our prior work.[12,28]

The finger was connected to a motorized stage (V-508 PIMag Precision Linear Stage, Physikinstrumente) by a Futek 250 g LSB force sensor (k = 48.2 kN m^{-1}, peak-to-peak noise of 0.1 mN) sampling at 550 Hz (Keithley 7510 DMM) to record traces of the frictional forces which the mock finger encountered while sliding across the surface. This sampling rate is similar to mechanoreceptor frequency.[45] During testing, the mock finger was first lowered at an angle until 1 cm × 1 cm square contact was made with the surface at the tip of the finger while the loading condition of mass, M, was applied. The force sensor was baselined to zero force. The finger was then pulled at a constant velocity, v, for 4 mm horizontally across the surface. Three subsequent pulls of the same mass, speed, and distance were then completed without separating the finger from the surface and were taken as data representative of the applied condition set. The first pull was not considered during testing due to the high likelihood of residual stresses or extraneous pressure simply present from setup with vertical initial contact and loading of applied mass M, as compared to the tangential stresses experienced during a sliding event. After the fourth pull was collected, the finger was lifted vertically off of the surface. This sequence was then repeated over two additional regions of the surface, to gather a total of nine representative friction traces for each testing condition (for a given M and v). This was then repeated for 16 combinations of M and v and performed on each of the two material surfaces.

Surface characterization

Successful deposition of silane coatings, coating integrity, and impact of repeated use were verified through four standard surface characterization techniques.

Contact angle hysteresis. A Kruss DSA14 srop shape analysis system goniometer was used to capture both advancing and receding water contact angles on sample surfaces. The advancing angle was captured by using a 30 μm tip syringe and micromanipulator to apply a ~2 μL droplet of DI water onto the sample until the drop visibly expanded on the surface. An image of the droplet was recorded for measurement of the advancing contact angle, and the droplet was subsequently retracted by the syringe until the drop visibly reduced on the surface. A second image was recorded as the receding contact angle. Five droplets were dispensed and their angles captured for each surface. The angle of each droplet at the surface was then measured by an automatic circle fit using ImageJ image processing software. Average advancing and receding angles were calculated and reported for each sample. The difference of values calculated for the individual droplets' advancing and receding angles was taken. The standard deviation of these differences is also reported for each sample.

Atomic force microscopy (AFM). Surface roughness and topological characterization of the card and applied surface coatings was performed using a Bruker Multimode AFM. 1 cm × 1 cm samples were analyzed by tapping mode scans over a 5 μm × 5 μm area at a rate of 1 Hz and drive frequency of 120 kHz. The profiles were then analyzed using Gwyddion software.

X-ray photoelectric spectroscopy (XPS). Elemental analysis of several card surfaces was performed *via* XPS of 1 cm × 1 cm samples. Spectra of the samples were gathered using a Thermo Scientific K-Alpha XPS system. The data were then analyzed using Thermo Scientific Avantage Data System software.

Fourier transform infrared spectroscopy (FTIR). 1 cm × 1 cm cutouts of card samples were used for Fourier transform infrared (FTIR) spectroscopy. All measurements were conducted on a PerkinElmer spectrum 100 FTIR spectrometer. Three measurements were taken of each sample to confirm whether the coating was homogeneous. To prevent cross-contamination, the probe was cleaned with ethanol prior to measurement of each sample. FTIR spectra were recorded from 4000 cm^{-1} to 600 cm^{-1}.

Human participants testing

Selection of blind and braille-literate participants

To determine the tactile discriminability of the two surfaces, human psychophysical testing was conducted with approval from the Institutional Review Board of the University of Delaware (Project #1773529) and thus in compliance with the Declaration of Helsinki. All participants gave informed consent to participate in the study. Training and evaluation *via* human participant testing was necessary for this work in order to provide empirical data assessing the materials' efficacy as tactile aids.[46] As we intended the materials and approach to be used in tactile aids for people who are severely visually impaired or blind, we selected for participants who were congenitally blind and braille-literate. While "blindness" is categorized as a single condition from a medical definition, it is itself a symptomatic reduction of conditions,[47,48] and the etiology is highly variable – from congenital to acquired, whether caused by brain injury or injury to the eye. Thus, a higher degree of variability is expected from participants who are blind as it is likely for participants to have different experiences, or even different perceptive processing.[49–53] To lower variability of participant experience, we selected for only congenitally blind participants. We also further selected for participants who were braille-literate to ensure that participants had a baseline tactile experience of interpreting information from their sense of touch.

Human participants were also tested in order to study the impact of repeated use, and potential wear or fouling, of the silane coatings. Vision capacity was not a selection criterion for the study on repeated use, as its primary objective was as an investigation into the response of the coatings to repeated frictional sliding contact of human fingers. Participants of both studies were compensated $20.

Task design

All study participants were first blindfolded to ensure consistency across physical and visual condition experienced during testing because it is possible for participants who are congenitally blind to have some residual visual cues of varying resolution.[54] After blindfolding, participants began an introductory familiarization stage, where they were given several freshly coated examples of ''type A'' (black/C4-APTMS) and ''type B'' (red/C5) cards. During this familiarization stage, participants were told the identity of the cards and were allowed to familiarize themselves with how the cards felt by freely exploring both types of cards without any time restriction or prescribed motions.

After familiarization, participants completed a training phase where they performed a two-alternative forced choice (2-AFC) task to determine card identity by touch, with feedback on whether the card they selected was correct. For each trial, participants were presented with one identified as ''type A'' (black/C4-ATMS) card and one ''type B'' (red/C5) card side-by-side, with their position to the participant's left or right randomized across trials. Participants were asked to identify which card was ''type A'' by freely exploring both cards by touch. After each trial, the participant was informed whether their selection was correct or incorrect before proceeding to the next trial. Running performance accuracy was calculated after the sixth trial, after which subsequent trials were performed until accuracy over the last six trials exceeded 66%. In principle, this training phase was capped at a maximum of twenty-five trials, after which the participant would move on to the testing phase even if they had not met the training accuracy threshold. However, all participants in the discriminability study exceeded 66% training accuracy prior to reaching the trial cap. Finally, in the testing phase of the study, participants performed 10 trials of the same 2-AFC task, without feedback.

Wear and durability

Wear *via* human participants

Additional human psychophysical testing was conducted to experimentally assess the durability of the silane surface coatings to physical wear. Sighted participants were blindfolded and completed the same familiarization, training, and testing phases as described above for coating discriminability. However, in this study, the testing phase was done using the same set of coated cards for all participants instead of fresh cards. That is, the first participant for durability testing was provided a freshly coated set of cards for their task, but the second participant was provided that same set of cards for their task after having already been used for 10 trails by the first participant. The third participant then used the cards after having been subjected to 20 trials, and the fourth after a total of 30 previous trials. Mechanical friction characterization, AFM, and FTIR samples of reliably worn surface areas were created by subjecting a prescribed area of a coated card to ten cycles of human finger frictional sliding contact.

Wear *via* mock finger for mechanical characterization

Separate samples of each coating were subjected to wear by either a real human finger or by the mock finger mechanical setup. The latter was performed by sliding the mock finger across the surface of the card for sixteen cycles. After the known area of the card surface was subjected to wear, mechanical friction characterization was then performed over the worn area. The same method as above was performed for collecting data of frictional traces, but it was performed for only a single condition of mass and velocity which had been previously deemed as having distinctive friction traces on fresh surfaces.

Results

Characterization of surface coatings

To coat the cards, the surfaces were first activated by UV-ozone ($UV\text{-}O_3$) and then the silane precursor was deposited onto the surface *via* through vacuum vapor-phase deposition, as described in the Methods. Successful deposition of *n*-butylaminopropyltrimethoxysilane (C4-APTMS) and *n*-pentyltrichlorosilane (C5) was confirmed through water contact angle, AFM, XPS, and FTIR (Fig. 2). The contact angle measurements of each silanized sample (Fig. 2a) followed a similar trend to a successful deposition on silicon substrate.[27,55] However, we do not expect an exact match in contact angles between cards and silicon due to the inherent roughness of the playing card surface. We observe a trend of increased hydrophobicity through their water contact angle measurements and hysteresis values (Table 1) from (62.6–74.4) $\pm$ 5.9° for the C4-APTMS card surface to (78.4–91.1) $\pm$ 5.1° for the C5 card surface, as expected. This follows the same trend of increasing hydrophobicity observed in pristine silicon samples from (56.8–72.7) $\pm$ 2.2° to (99.8–106.9) $\pm$ 1.5° for pristine, perceptibly smooth silicon wafer substrates silanized with C4-APTMS and C5, respectively.[27] The C4-APTMS sample has a similar surface energy to that of the $UV\text{-}O_3$ treatment, but there exist notable differences in their topography by AFM to evidence successful surface coating.

AFM topographies (Fig. 2b) over 5 μm × 5 μm areas showed a difference in surface features and their distribution across each silane coating, as compared to the uncoated card which was simply subjected to $UV\text{-}O_3$ treatment. Large aggregate features in C4-APTMS, and smaller aggregates present in the C5 sample at higher frequency, were seen to closely resemble those previously reported by Oyola-Reynoso *et al.*[42] They found that in cellulose substrates, such as those used in the present study, the aggregates are more likely to form by utilizing

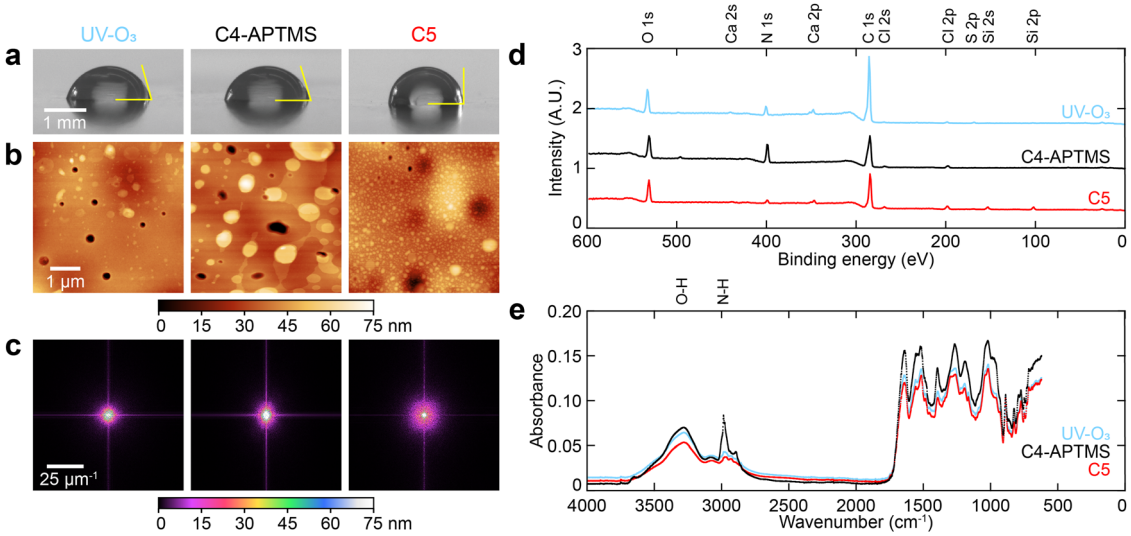

Fig. 2 Materials characterization of card surfaces. (a) Water contact angle of activated surface prior to silane deposition (UV-O_3) and the two different surfaces upon successful deposition (C4-APTMS and C5). (b) Height profiles of samples obtained by AFM. (c) FFT representation of AFM surface topography to visualize ordering. (d) Relative intensity of XPS signal (see Table 1), with samples normalized to have equal oxygen peak intensities. (e) Data obtained by FTIR of fresh examples of each sample.

Table 1 Surface coatings and properties

Sample	Chemical structure	Contact angle (°)	Roughness, R_a (nm)	Hurst exponent, H	C 1s (%)	O 1s (%)	N 1s (%)	Si 2p (%)	Ca 2p (%)	S 2p (%)	Cl 2p (%)
UV-ozone (UV-O_3)	—	(66.5–75.2) ± 5.6	3.71	0.51	77.8	12.7	6.6	—	1.6	0.7	0.6
n-Butylaminopropyltrimethoxysilane (C4-APTMS)	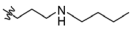	(62.6–74.4) ± 5.9	6.36	0.58	64.3	15.6	18.0	—	—	—	1.3
n-Pentyltrichlorosilane (C5)		(78.4–91.1) ± 5.1	5.41	0.84	68.9	17.6	4.1	5.0	1.4	—	2.7

adsorbed water within the cellulose substrate to enable a step-growth polymerization over those regions. This reaction creates a chain of siloxane bonds over water-rich regions, similar to those binding the monolayered areas to the surface. These aggregates are less frequently observed when depositing silanes onto silicon substrates.[27,56] However, this additional roughness introduced by potentially polymerized non-monolayer regions was not a cause of concern in the study here as the card surfaces are already perceptibly rough,[34] and our focus was to determine if everyday objects which are already perceptibly rough could generate distinctive tactile feedback based on surface coating with different chemistries. The fast Fourier transform (FFT) of the topography (Fig. 2c) also quantifies surface differences between C4-APTMS and C5 through evaluation in the spatial frequency domain. The more diffuse signal from the C5 sample demonstrates a difference in roughness scaling behavior compared to C4-APTMS.[57] The power spectrum density (PSD) can be utilized to quantify this difference in surface features and spatial distribution of roughness.[58] The slope of the linear regime on a log(PSD) *versus* log(spatial frequency) plot (see S1 in the ESI†) can be used to calculate the Hurst exponent (H), a roughness scaling factor, as $H = 1 + 0.5 \times (|\text{slope}|)$ which describes how the surface roughness changes with scale.[59,60] The Hurst exponent was higher for the C5 sample than for C4-APTMS (Table 1), indicating the C5 sample has greater changes in surface roughness upon scaling, *i.e.* smoother features at smaller length scales. The lower Hurst exponent for C4-APTMS indicates a more similar roughness at all length scales. A high Hurst exponent has been correlated with a more disordered surface due to the smoothing effect on the surface at nano length scales, while a lower Hurst exponent has been correlated with a more ordered layer as it maintains a roughness similar to the underlying substrate, preserving a more self-affine topography.[27] In summary, C4-APTMS shows visually larger feature sizes (polymerized aggregates) than C5, and the higher H for C5 indicates larger differences in roughness at nano length scales and a more molecularly disordered layer compared to the C4-APTMS surface.

The XPS spectra (Fig. 2d) obtained from each sample were normalized to have equal maximum signal intensity at their oxygen 1s peaks (532 eV).[61] The signal peaks produced at 400 and 285 eV were analyzed to verify the addition of silanes, as they correspond to the binding energies of nitrogen and carbon, respectively.[61] We saw that the C4-APTMS surface coating contained an increase in nitrogen as compared to the C5 (Table 1), but that the two had similar carbon signals. The nitrogen signal strengths provided evidence of successful formation of the C4-APTMS coating, due to the amine group

introduced in its structure. However, while there are alkyl groups present at the surface in both coatings, C4-APTMS contains two additional carbons in its structure. Similar carbon signal from both may suggest that the amine group of C4-APTMS had attenuated signal from elements closer to the card interface. Unlike typical substrates like silicon wafers, we saw additional peaks in the UV-O_3 and C5 samples. Peaks in the UV-O_3 and C5 samples at 349 and 439 eV indicated a presence of calcium.[61] This could be due to $CaCO_3$, a commonly used compound in white pigmentation,[62] in the card. This peak, however, was not present in the C4-APTMS signal, which may be due to signal attenuation. The binding energy peaks which were present in the C5 signal at 153 and 102 eV indicated presence of silicon,[61] which was expected from the silane-based surface coatings.

In addition to XPS, we also utilized FTIR to confirm successful silanization and surface coating formation. From the FTIR results (Fig. 2e), we observed a sharp N–H stretch in the C4-APTMS sample at 2950–2980 cm^{-1}.[63] This strong amine peak in the C4-APTMS sample, but not in the UV-O_3 and C5 samples, bolsters the XPS result for successful C4-APTMS surface coating formation over the card surface. The C5 sample did present a broader peak from 2840–3000 cm^{-1},[64] indicative of its alkyl group. Finally, we also saw a strong and broad peak from 3200 to 3550 cm^{-1} in all samples. This is indicative of an O–H, which may suggest adsorbed water.[65] However, it may also indicate the presence of hydroxyl groups, which facilitate covalent bonding of silanes to the surface.[66] This may explain why the chosen brand cards was more successful in achieving silanization than the other brands of cards, which lacked this O–H peak in their FTIR spectra (see S2 in ESI†), due to unknown differences in their proprietary surface coating formulation.

Mechanical characterization with mesoscale sliding friction

Despite our surface characterization, there is no single material property or parameter which can predict whether humans can distinguish surfaces based on chemical structure. Adding to this difficulty, mesoscale friction forces are well-known to depend on the applied load and sliding velocity,[67] both of which vary during free exploration by humans. To confirm that these surfaces are likely to be useful as a tactile aid prior to testing with humans, and to quantitatively investigate the effects of wear in later sections, we performed mesoscale mechanical friction tests. Following a previously established protocol,[11,28] we performed mechanical friction testing on the cards using a "mock finger" made from PDMS. (Fig. 3a, with further details and justification in the methods). The PDMS was then surface oxidized using long-term exposure to UV-O_3 to ensure a non-sticky surface, and several of the physiochemical and geometric properties of the mock finger were selected to model the human finger.[12,27,28] The mock finger was weighed and found to be 5.2 g, and was then slid at several different

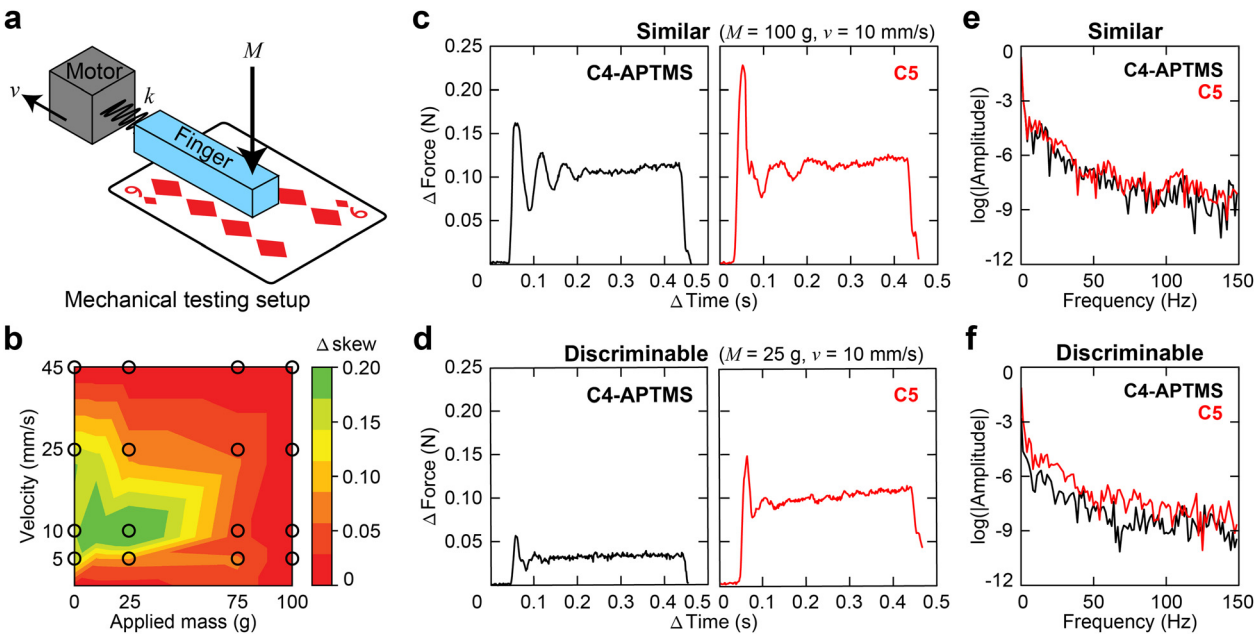

Fig. 3 Mechanical characterization of card coatings by friction. (a) Schematic of testing apparatus which measures friction forces from a force sensor, with spring constant *k*, of a mock finger as it slides across cards at different combinations of sliding velocity, *v*, as set by a linear actuator and applied mass, *M*. Zero applied mass implies no added mass apart from the deadweight of mock finger (5.2 g). (b) Representative friction force traces of a mock finger sliding on a card coated with C5 or C4-APTMS at one combination of *M* and *v* which did not result in "discriminable" force traces, as quantified by the skew of the cross-correlation. (c) FFT of the friction traces in panel b which were not deemed "discriminable." (d) "Discriminability matrix" which shows combinations of *M* and *v* where C5 and C4-APTMS feel distinctive from one another and were deemed "discriminable," as quantified by the skew of the cross-correlation. (e) Representative friction force traces of a mock finger sliding on a card coated with C5 or C4-APTMS at a combination of *M* and *v* which resulted in "discriminable" force traces, as quantified by the skew of the cross-correlation. (f) FFT of the friction traces in panel b which were deemed "discriminable."

velocities (5, 10, 25, 45 mm s^{-1}) and applied loads (0, 25, 75, 100 g in addition to the deadweight of the mock finger) to mimic the range of human exploration.[27]

Representative friction traces from mechanical testing of each surface for different mass, M, and velocity, v, conditions are shown in Fig. 3c and d. The friction traces shown in Fig. 3c were obtained at a condition (v = 10 mm s^{-1}, M = 100 g) found to produce similar traces. Here, similarity is quantified by cross-correlating the vectors and computing the differences in their skews. Fig. 3d shows friction traces of each surface at a condition which was deemed "discriminable," having a greater difference in skew. We observe mechanical features such as singular stiction spikes at the onset of sliding (C5) and dampening slow frictional waves (Fig. 3c), which occur for longer periods throughout a trace.[67,68] These are examples of mechanical instabilities which arise from the competition between elasticity and adhesion.[21] On the same surfaces, but at a different combination of M and v, Fig. 3d shows a condition (v = 10 mm s^{-1}, M = 25 g) where the two surfaces lead to friction forces that may be discriminable. This difference highlights the challenge of predicting human performance based on the dynamic process of friction. Both traces in this comparison contain oscillations that dampen throughout the trace at similar frequencies, but only C5 shows larger periodicity above electronic noise. These disparities, in addition to the visibly different magnitudes, suggest that these coatings, even on rough playing cards, could lead to noticeably different tactile perception in a tactile aid. A "discriminability matrix," shown in Fig. 3b, summarizes the masses and velocities which lead to either similar or discriminable friction from the two surfaces, as quantified by cross-correlation. We previously found that this method of categorization was more predictive of human behavior than using an average value of friction (*i.e.*, an average friction coefficient) or any material property, such as those in Fig. 2.[28] Conditions which produced frictional data across the two materials that were quantified to be more different may provide exploratory conditions at which the two surfaces are more distinguishable to humans during free exploration.

Vibrational frequencies, brought about by microscale stick-slip adhesion at the interface, give detail to touch as one explores the tactile qualities of an object.[11,69] Time-dependent signals have also been studied elsewhere for touch and analyzed in the Fourier domain.[70,71] We analyzed the data here by FFT to seek whether the microscale adhesive vibrations encountered during sliding at a discriminable condition would produce more prominent signal differences over the frequency domain. In Fig. 3e, more regions of overlap are seen when comparing the similar traces, while in traces which are discriminable, C5 and C4-APTMS have visible differences at most frequencies (Fig. 3f). The C4-APTMS trace in Fig. 3d does not exhibit slow frictional waves and has a consistently lower value across the Fourier domain. At both conditions, C5 is the higher stiction surface, but stiction being a single event makes this feature less recognizable in the frequency domain. No significant deviation in the FFT

Fig. 4 Card identification by coatings with human participants. (a) Overview schematic of the psychophysical study. Participants were provided with black-suited and red-suited playing cards which had been silanized with C4-APTMS and C5, respectively. After familiarization and training stages, participants completed a two-alternative forced choice (2-AFC) test to identify the cards by touch. (b) Picture of the 2-AFC task. (c) Average accuracy of the 2-AFC test per participant. Mean accuracy of all participants was 82% (solid dark blue line), as compared to chance performance of 50% (dashed red line). 95% confidence interval, calculated by Wilson score, is shaded in gray.

data appears at values that would correspond to electronic noise of the instrument, (*e.g.* 60 Hz, 120 Hz) so the data obtained during steady sliding has real mechanical origin. The consistent differences in the FFT across broad ranges of frequencies suggests that stiction alone might not drive tactile discriminability. Although mechanoreceptors in the finger are known to be sensitive to certain frequencies,[34,69,72,73] no mechanistic connection between FFT signals by mechanical testing and human performance by fine touch has been established, and the work is ongoing in the field.[20,28,71,74]

Human participants testing

We performed human psychophysical testing with study participants (project #1773529) to determine if humans can identify objects coated with these silanes in practice. Five congenitally blind and braille-literate participants were provided silanized playing cards, with one silane representing black-suited cards (C4-APTMS) and another representing red-suited cards (C5), and tested on whether they could accurately identify them by touch alone. An overview of the study is provided in Fig. 4a. Participants were provided several examples of freshly coated cards identified to be "type A" (black/C4-APTMS) and "type B" (red/C5), and allowed to freely explore and familiarize themselves with each type. They were then trained in a two-alternative forced choice (2-AFC) task, where they were presented with one of each type of card randomly positioned to either their "left" or "right," and asked to identify which one was "type A." During this training, participants were provided feedback as to whether their selection was correct or incorrect. After achieving a 66% accuracy threshold, participants performed 10 trials of the 2-AFC task during the testing portion of the study without feedback, which was used to calculate individual performance accuracy (see Fig. 4c).

The total of all participant testing (n = 50 trials) gave a mean accuracy of 82%, with performance significantly better than chance (one-sample t-test, $t(4) = 3.30$, $p < 0.05$). At an individual level, three out of five participants responded significantly better than chance (binomial tests, $p < 0.05$). One participant scored equal to chance, but this participant noted they had difficulty with the recollection aspect of the test. They specifically gave feedback that they sometimes forgot which texture corresponded to "A" or "B." In instances demonstrating success, one participant (who achieved 100% accuracy) successfully self-corrected during the test, whereby they had initially identified a card incorrectly, but reconsidered and changed their choice to the correct card. Another participant who also

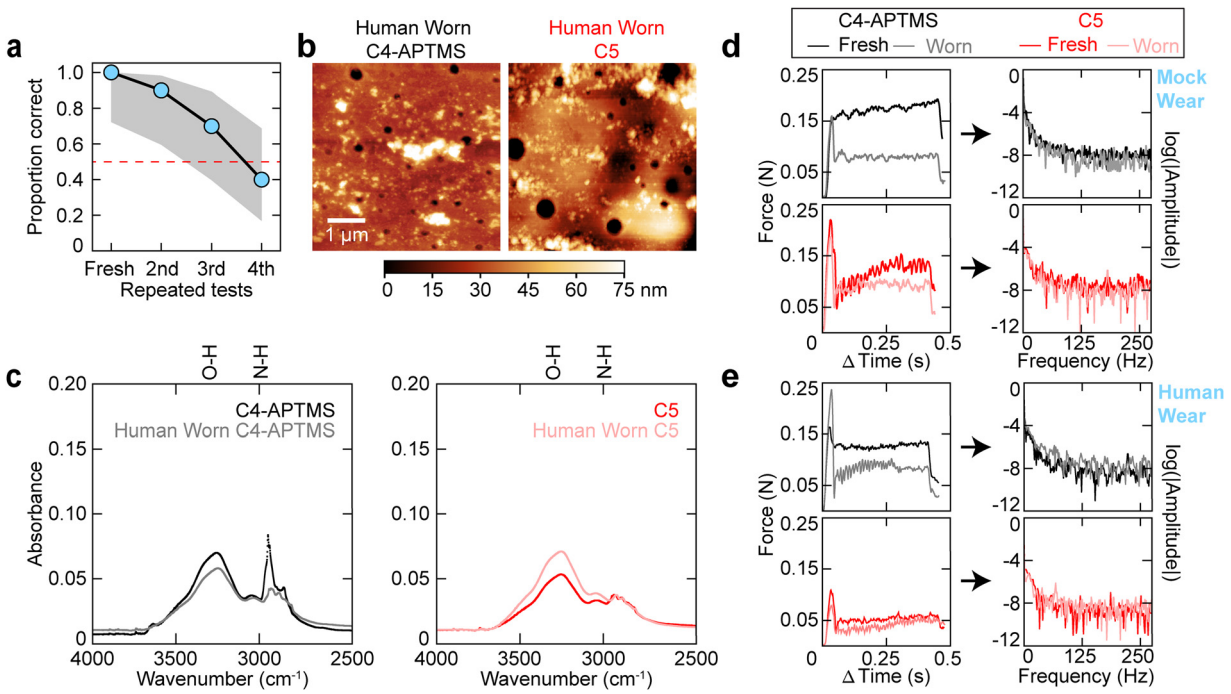

Fig. 5 Durability of coatings to human or mechanical wear. (a) 2-AFC test of 10 card pairs by participants, repeated using the same set of cards. Chance performance of 50% is shown as the dashed red line, and 95% confidence intervals given by Wilson score intervals are shaded gray for each participant. (b) Height profiles obtained by AFM of samples worn by a human finger. (c) Data obtained by FTIR of O–H and N–H stretches in samples worn by a human finger compared to that of fresh coatings. (d) Mechanical characterization with mock finger, over the same area of a card as worn by the mock finger itself, at M = 25 g and v = 10 mm s^{-1}. The left column shows friction traces recorded from mock-worn samples compared to that of the fresh coatings. Darker traces represent data collected from a fresh spot. Measurement performed for a total of 16 times, and worn trace is of the last collected measurement. The FFT of each friction trace can be seen in the right column. (e) Mechanical characterization with mock finger, over the same area of a card previously worn by a human finger, at M = 25 g and v = 10 mm s^{-1}. The left column shows friction traces recorded from human-worn samples compared to that of fresh coatings, and darker traces represent data collected from a fresh spot. The FFT of each friction trace can be seen adjacent in the right column.

achieved 100% accuracy was able to perform the test as rapidly as the test administrator could provide the cards, indicating support for these surface coatings as a method to generate distinct textures in a tactile aid. We also confirmed that uncoated cards were not discriminable by participants in S3 of the ESI.†

Impact of mechanical wear

In all experiments prior to this section, we used freshly coated cards to ensure consistent surface chemistry. This approach controlled for potential surface fouling and mechanical wear from participant use, which may have varied the tactile stimuli experienced by later participants. As these impacts were excluded during the above testing and characterization, it was important to additionally investigate potential impact of wear and fouling upon repeated use. Surface fouling and wear were analyzed using mechanical characterization, surface characterization, and with human participants. The mechanical and surface techniques were identical to those used before, but we had small modifications for human testing. In the task here, the first participant was asked to distinguish a set of fresh cards, but the same set of cards was then used to test a second, third, and then fourth participant (Fig. 5a). We found that participant accuracy decreased with repeated use, with the first participant scoring 10/10 and the last participant only achieving 4/10, despite training. We found that the 75% mean participant accuracy of this study that re-used cards was not significantly better than chance (one-sample *t*-test, $t(3) = 1.89$, $p > 0.05$, not significant), and we see a statistically significant decline between participant accuracy and the repeated use of cards over multiple tests (Fisher's exact, $p < 0.05$).

Significant differences in surface features were seen after the coatings were subjected to repeated wear. AFM of samples worn by a human finger (Fig. 5b) showed a loss of notable aggregate features which had been present in fresh samples. To characterize if wear reduced differences in the friction between the two surfaces – which would lead to a lower ability to distinguish the two surfaces by touch – we repeated mechanical testing on the same spot on each card. This is in contrast to the testing performed earlier in Fig. 4, which was always performed on fresh areas of the surface. After a pull was collected over a fresh spot, 15 more pulls on the same spot followed. This wear was performed in two ways: either with a mock finger or with a human finger to observe the effects of finger residue. Unlike in the earlier mechanical testing, frictional testing was performed at a single condition (v = 10 mm s^{-1} and M = 25 g) since this condition had been previously deemed "discriminable" by the skew of cross-correlation for fresh samples in order to examine whether repeated wear reduced the difference between the surfaces' friction traces.

Wear by humans *versus* wear performed by the mock finger had differing impacts on C4-APTMS and C5. With both wear by the mock finger and by human fingers (Fig. 5d and e, right column), a stiction spike appears or becomes more prominent. This suggests that C4-APTMS suppressed a stiction spike, but with wear, the reappearance of a stiction spike makes C4-APTMS more similar to the C5 friction trace, as C5 always presents a stiction spike, regardless of wear. Stiction having a singular occurrence at the beginning of a friction trace makes it difficult to capture in the frequency domain. With human wear, the friction signals in C5 and C4-APTMS also appear to become more similar. The steady sliding of C4-APTMS and the punctuated smaller oscillations in C5 both evolved towards regular oscillations with wear. Evidence of this appears in the frequency space, in the form of a small, positive vertical shift of human-worn C4-APTMS across most frequencies.

FTIR analysis was performed on samples of each card's surface coating which had been mechanically worn by a human finger and compared to that of freshly coated samples (Fig. 5c). As in the FTIR spectra of the freshly coated cards above, both human-worn surface coatings showed a significant O–H stretch signal after repeated use. Furthermore, after being subjected to wear, the C5 coating of the red cards was seen to produce results similar to its fresh state, retaining its 2840–3000 cm^{-1} alkane peak. The worn C4-APTMS coating of the black-suited cards also presented an alkane peak, however, it showed a loss of the prominent 2950–2980 cm^{-1} amine peak that had been present in the fresh sample. XPS characterization of the samples worn by a human finger (see S2 in ESI†) additionally showed evidence of fouling. Signal peaks were produced from the Na 1s 1071 eV binding energy[61] as well as that of K 2p at 294 eV.[61] These results were both attributed to surface fouling from the human finger, as both sodium and potassium are known exudates of human skin.[75]

FTIR and mechanical testing both suggest that C4-APTMS is being degraded more significantly than C5. By FTIR, the remaining peak, suggestive of short alkyl groups in C4-APTMS, indicates that the wear may have mechanically cleaved at the amine group. This material loss may be due to hydrolysis of the amine group, which is known to occur in other works.[76–78] After this removal, both card coatings presented an alkyl group at the surface, and both coatings are seen to have similar FTIR signals after being subjected to wear. This result bolsters that of the FFT of frictional forces and AFM of the worn surfaces to suggest that the C4-APTMS coating experienced significant wear upon repeated frictional sliding contact, while the C5 coating did not. In short, the C4-APTMS coating becomes more like C5 with wear. These results (Fig. 5a) provide a mechanistic explanation for the reduction in performance of human participants.

Discussion

Overall, blind users were able to use silane coatings as a method to distinguish between black- and red-suited cards. Despite the inherent roughness of playing cards, the frictional differences from surface chemistry of C4-APTMS and C5 still provided a sufficiently strong cue. Previously, these surface modifications were only demonstrated on pristine, smooth silicon wafers. Thus, in this work, the surface coatings provided a sufficiently salient signal as applied onto a perceptibly rough

surface and were not overwhelmed by its underlying physical features, demonstrating their use on everyday surfaces. However, given the complexity of mesoscale friction, it is not clearly established that smooth surfaces are, in principle, better or worse at accentuating differences in surface chemistry. Ultimately, given a relatively short training, several users were able to rapidly distinguish surface coatings, and likely this accuracy and speed would be seen in more participants with more training, which would be the case of a tactile aid in everyday use.

Our results also indicate that the C4-APTMS surface coating experienced wear, which reduces the potential of C4-APTMS as a user-ready coating. However, we highlight that the goal of this paper was to demonstrate the basic principle that surface chemistry could impart distinctive tactile cues as an assistive aid. More durable coatings in the future could be a composite or polymer, but starting with composites or polymers here would make it difficult to establish insights into the minimal chemical feature changes required to create surfaces that feel different. Additionally, the object's inherent surface chemistry may be left unmodified to serve as a tactile comparison against a single material coating. Our methodology to investigate wear gave mechanistic support for why C4-APTMS lost its performance over repeated use. The wear experiments also helped reveal some insights at the longstanding challenge of correlating friction forces to human tactile performance. For example, we saw that the stiction spike, though prominent in a friction curve, may be more useful as a classifier rather than the details of its magnitude. Loss of the amine group in worn C4-APTMS surfaces, left a short chain alkyl group at its surface similar to C5. We saw that C4-APTMS, upon wear, began to form a stiction spike, and that this stiction spike was different in magnitude over a slightly different duration than that of C5. The simplest explanation for why worn C4-APTMS and C5 surfaces felt the same was because they were left with similar surface chemistries after repeated use and both exhibited a stiction spike, whereas fresh C4-APTMS exhibits steady sliding.

Conclusions

The silane coatings used here provided distinctive tactile feedback to the user, even when coated on the perceptibly rough playing card surface. The C4-APTMS surface coating, however, lacked the durability necessary to retain that discriminability over repeated use. The fact that participants were provided training during the studies was not seen as a particular disadvantage of the platform, as some form of training is expected in most forms of information acquisition, whether in braille literacy or even with visual scientific plots. In practice, especially in application on a tactile graphic, a legend is often utilized as a reference touchpoint for tactile translation or an established convention is employed to indicate meaning. Thus, if participants were continually using these surface coatings, then the familiarity may lead to more rapid interpretation and higher accuracy across most users.

While there exist blind-accessible objects such as playing cards that use bumps or braille, the embossed bumps may also abrade, are visually apparent to sighted peers which is bad in a competitive game, and coatings are inherently easier to integrate with industrial-scale manufacture. Indeed, the cards already have a surface coating applied to them. The current state of purely physically featured tactile graphics does not fully leverage modern advances in materials engineering. Next-generation tactile aids that employ both physical and chemical features simultaneously in a single assistive aid may increase information density and processing bandwidth without confusion from tactile clutter. The results, methodology, and material considerations communicated here develop the understanding of materials in tactile perception, and offer progress in information accessibility for those who are severely visually impaired or blind.

Data availability

3D modelled tactile graphics of all figures presented in this work are also available for download through the ESI.† Data supporting this article can be found throughout or in the ESI.†

Conflicts of interest

The authors have filed the work here in a provisional patent (US 63/617,093).

Acknowledgements

We acknowledge support from the National Eye Institute of the National Institutes of Health under award number R01EY032584. We acknowledge the National Federation of the Blind for consultation. L. V. K. acknowledges support from the Beckman Young Investigator award from the Arnold and Mabel Beckman Foundation. AFM was conducted at the Delaware Biotechnology Institute's Bio-Imaging Center at the University of Delaware, and the instrumentation was supported by NIH-NIGMS (P20GM103446) as well as the State of Delaware. XPS was conducted at the University of Delaware's Surface Analysis Facility with instrumentation sponsored by the National Science Foundation (CHE-1428149). FTIR was conducted at the University of Delaware's Advanced Materials Characterization Lab. Participants. Studies involving human participants were approved by the Institutional Review Board of the University of Delaware (Project #1773529). Data were collected from a total of 9 healthy volunteers between the ages of 18 and 50.

References

1 E. E. Pissaloux, R. Velázquez and F. Maingreaud, A New Framework for Cognitive Mobility of Visually Impaired Users in Using Tactile Device, *IEEE Trans. Hum.-Mach. Syst*, 2017, **47**(6), 1040–1051.
2 L. E. Magee and J. M. Kennedy, Exploring Pictures Tactually, *Nature*, 1980, **283**(5744), 287–288, DOI: **10.1038/283287a0**.

3 J. M. Kennedy and J. Bai, Haptic Pictures: Fit Judgments Predict Identification, Recognition Memory, and Confidence, *Perception*, 2002, **31**(8), 1013–1026, DOI: **10.1068/p3259**.
4 D. T. V. Pawluk, R. J. Adams and R. Kitada, Designing Haptic Assistive Technology for Individuals Who Are Blind or Visually Impaired, *IEEE Trans. Haptics*, 2015, **8**(3), 258–278, DOI: **10.1109/TOH.2015.2471300**.
5 A. M. Brock, P. Truillet, B. Oriola, D. Picard and C. Jouffrais, Interactivity Improves Usability of Geographic Maps for Visually Impaired People, *Hum. Comput. Interact.*, 2015, **30**(2), 156–194, DOI: **10.1080/07370024.2014.924412**.
6 Guidelines and Standards for Tactile Graphics. **https://www.brailleauthority.org/tg/**.
7 K. M. Gomes, S. T. Reeves and S. L. Riggs, The Evaluation of Tactile Parameters and Display Prototype to Support Physiological Monitoring and Multitasking for Anesthesia Providers in the Operating Room, *IEEE Trans. Haptics*, 2020, **13**(3), 628–644, DOI: **10.1109/TOH.2019.2960017**.
8 M. Langelaan, M. R. de Boer, R. M. A. van Nispen, B. Wouters, A. C. Moll and G. H. M. B. van Rens, Impact of Visual Impairment on Quality of Life: A Comparison With Quality of Life in the General Population and With Other Chronic Conditions, *Ophthalmic Epidemiol.*, 2007, **14**(3), 119–126, DOI: **10.1080/09286580601139212**.
9 D. M. Taylor, *Americans With Disabilities: 2014 Household Economic Studies Current Population Reports*, 2018, **https://factfinder.census.gov**.
10 C. Kirchner and B. Smith, Transition to What? Education and Employment Outcomes for Visually Impaired Youths after High School, *J. Vis. Impair. Blind.*, 2005, **99**(8), 499–504, DOI: **10.1177/0145482X0509900806**.
11 C. W. Carpenter, C. Dhong, N. B. Root, D. Rodriquez, E. E. Abdo, K. Skelil, M. A. Alkhadra, J. Ramírez, V. S. Ramachandran and D. J. Lipomi, Human Ability to Discriminate Surface Chemistry by Touch, *Mater. Horiz.*, 2018, **5**(1), 70–77, DOI: **10.1039/C7MH00800G**.
12 C. Dhong, L. V. Kayser, R. Arroyo, A. Shin, M. Finn, A. T. Kleinschmidt and D. J. Lipomi, Role of Fingerprint-Inspired Relief Structures in Elastomeric Slabs for Detecting Frictional Differences Arising from Surface Monolayers, *Soft Matter*, 2018, **14**(36), 7483–7491.
13 A. J. Gellman and N. D. Spencer, Surface Chemistry in Tribology. in *Wear – Materials, Mechanisms and Practice*, ed. G. W. Stachowiak, Wiley, 2005, pp. 95–122, DOI: **10.1002/9780470017029.ch6**.
14 R. Varma, T. S. Vajaranant, B. Burkemper, S. Wu, M. Torres, C. Hsu, F. Choudhury and R. McKean-Cowdin, Visual Impairment and Blindness in Adults in the United States, *JAMA Ophthalmol.*, 2016, **134**(7), 802, DOI: **10.1001/jamaophthalmol.2016.1284**.
15 M. Mukhiddinov and S.-Y. Kim, A Systematic Literature Review on the Automatic Creation of Tactile Graphics for the Blind and Visually Impaired, *Processes*, 2021, **9**(10), 1726.
16 L. Race, C. Fleet, D. Montour, L. Yazzolino, M. Salsiccia, C. Kearney-Volpe, S. Wells-Jensen and A. Hurst, Designing While Blind: Nonvisual Tools and Inclusive Workflows for Tactile Graphic Creation, *The 25th International ACM SIGACCESS Conference on Computers and Accessibility*, ACM, New York, NY, USA, 2023, pp. 1–8, DOI: **10.1145/3597638.3614546**.
17 M. Sreelakshmi and T. D. Subash, Haptic Technology: A Comprehensive Review on Its Applications and Future Prospects, *Mater. Today Proc.*, 2017, **4**(2), 4182–4187.
18 S. Biswas and Y. Visell, Emerging Material Technologies for Haptics, *Adv. Mater. Technol.*, 2019, **4**(4), 1900042, DOI: **10.1002/admt.201900042**.
19 V. R. Schinazi, T. Thrash and D. Chebat, Spatial Navigation by Congenitally Blind Individuals, *WIREs Cogn. Sci.*, 2016, **7**(1), 37–58, DOI: **10.1002/wcs.1375**.
20 D. J. Lipomi, C. Dhong, C. W. Carpenter, N. B. Root and V. S. Ramachandran, Organic Haptics: Intersection of Materials Chemistry and Tactile Perception, *Adv. Funct. Mater.*, 2020, **30**(29), 1906850, DOI: **10.1002/adfm.201906850**.
21 C. J. Rand and A. J. Crosby, Friction of Soft Elastomeric Wrinkled Surfaces, *J. Appl. Phys.*, 2009, **106**(6), 064913, DOI: **10.1063/1.3226074**.
22 R. H. Fast and C. J. Schwartz, A Study of the Role of Surface Parameters on the Relationship between Biotribology and Cognitive Perception Involved in the Design of Tactile Graphics, *Wear*, 2023, **523**, 204877.
23 M. W. A. Wijntjes, T. Van Lienen, I. M. Verstijnen and A. M. L. Kappers, The Influence of Picture Size on Recognition and Exploratory Behaviour in Raised-Line Drawings, *Perception*, 2008, **37**(4), 602–614, DOI: **10.1068/p5714**.
24 M. Wong, V. Gnanakumaran and D. Goldreich, Tactile Spatial Acuity Enhancement in Blindness: Evidence for Experience-Dependent Mechanisms, *J. Neurosci.*, 2011, **31**(19), 7028–7037, DOI: **10.1523/JNEUROSCI.6461-10.2011**.
25 J. M. Loomis, R. L. Klatzky and N. A. Giudice, Sensory Substitution of Vision: Importance of Perceptual and Cognitive Processing, *Assistive technology for blindness and low vision*, CRC Press, 2018, pp. 179–210.
26 S. J. Lederman and R. L. Klatzky, *Relative Availability of Surface and Object Properties During Early Haptic Processing*, 1997, vol. 23, pp. 1680–1707.
27 A. Nolin, A. Licht, K. Pierson, C.-Y. Lo, L. V. Kayser and C. Dhong, Predicting Human Touch Sensitivity to Single Atom Substitutions in Surface Monolayers for Molecular Control in Tactile Interfaces, *Soft Matter*, 2021, **17**(19), 5050–5060.
28 A. Nolin, K. Pierson, R. Hlibok, C.-Y. Lo, L. V. Kayser and C. Dhong, Controlling Fine Touch Sensations with Polymer Tacticity and Crystallinity, *Soft Matter*, 2022, **18**(20), 3928–3940.
29 N. H. Runyan and D. B. Blazie, The Continuing Quest for the ''Holy Braille'' of Tactile Displays, in *Nano-Opto-Mechanical Systems (NOMS)*, ed. J. Esteve, E. M. Terentjev and E. M. Campo, SPIE, 2011, vol. 8107, p. 81070G, DOI: **10.1117/12.897382**.
30 K. Ren, S. Liu, M. Lin, Y. Wang and Q. M. Zhang, A Compact Electroactive Polymer Actuator Suitable for Refreshable Braille Display, *Sens. Actuators Phys.*, 2008, **143**(2), 335–342.

31 G. Frediani, J. Busfield and F. Carpi, Enabling Portable Multiple-Line Refreshable Braille Displays with Electroactive Elastomers, *Med. Eng. Phys.*, 2018, **60**, 86–93, DOI: 10.1016/j.medengphy.2018.07.012.

32 N. Torras, K. E. Zinoviev, C. J. Camargo, E. M. Campo, H. Campanella, J. Esteve, J. E. Marshall, E. M. Terentjev, M. Omastová, I. Krupa, P. Teplický, B. Mamojka, P. Bruns, B. Roeder, M. Vallribera, R. Malet, S. Zuffanelli, V. Soler, J. Roig, N. Walker, D. Wenn, F. Vossen and F. M. H. Crompvoets, Tactile Device Based on Opto-Mechanical Actuation of Liquid Crystal Elastomers, *Sens. Actuators Phys.*, 2014, **208**, 104–112, DOI: 10.1016/j.sna.2014.01.012.

33 F. Sorgini, R. Caliò, M. C. Carrozza and C. M. Oddo, Haptic-Assistive Technologies for Audition and Vision Sensory Disabilities, *Disabil. Rehabil. Assist. Technol.*, 2018, **13**(4), 394–421, DOI: 10.1080/17483107.2017.1385100.

34 L. Skedung, M. Arvidsson, J. Y. Chung, C. M. Stafford, B. Berglund and M. W. Rutland, Feeling Small: Exploring the Tactile Perception Limits, *Sci. Rep.*, 2013, **3**(1), 2617, DOI: 10.1038/srep02617.

35 A. Lio, D. H. Charych and M. Salmeron, Comparative Atomic Force Microscopy Study of the Chain Length Dependence of Frictional Properties of Alkanethiols on Gold and Alkylsilanes on Mica, *J. Phys. Chem. B*, 1997, **101**(19), 3800–3805, DOI: 10.1021/jp963918e.

36 E. Barrena, S. Kopta, D. F. Ogletree, D. H. Charych and M. Salmeron, Relationship between Friction and Molecular Structure: Alkylsilane Lubricant Films under Pressure, *Phys. Rev. Lett.*, 1999, **82**(14), 2880–2883, DOI: 10.1103/PhysRevLett.82.2880.

37 S. Niederberger, D. H. Gracias, K. Komvopoulos and G. A. Somorjai, Transitions from Nanoscale to Microscale Dynamic Friction Mechanisms on Polyethylene and Silicon Surfaces, *J. Appl. Phys.*, 2000, **87**(6), 3143–3150.

38 F. Geyer, M. D'Acunzi, A. Sharifi-Aghili, A. Saal, N. Gao, A. Kaltbeitzel, T.-F. Sloot, R. Berger, H.-J. Butt and D. Vollmer, When and How Self-Cleaning of Superhydrophobic Surfaces Works, *Sci. Adv.*, 2020, **6**(3), eaaw9727, DOI: 10.1126/sciadv.aaw9727.

39 O. Ben-David and J. Fineberg, Static Friction Coefficient Is Not a Material Constant, *Phys. Rev. Lett.*, 2011, **106**(25), 254301, DOI: 10.1103/PhysRevLett.106.254301.

40 W. Tang, N. Chen, J. Zhang, S. Chen, S. Ge, H. Zhu, S. Zhang and H. Yang, Characterization of Tactile Perception and Optimal Exploration Movement, *Tribol. Lett.*, 2015, **58**(2), 28, DOI: 10.1007/s11249-015-0507-4.

41 A. Vanossi, D. Dietzel, A. Schirmeisen, E. Meyer, R. Pawlak, T. Glatzel, M. Kisiel, S. Kawai and N. Manini, Recent Highlights in Nanoscale and Mesoscale Friction, *Beilstein J. Nanotechnol.*, 2018, **9**(1), 1995–2014.

42 S. Oyola-Reynoso, I. D. Tevis, J. Chen, B. S. Chang, S. Çinar, J.-F. Bloch and M. M. Thuo, Recruiting Physisorbed Water in Surface Polymerization for Bio-Inspired Materials of Tunable Hydrophobicity, *J. Mater. Chem. A*, 2016, **4**(38), 14729–14738, DOI: 10.1039/C6TA06446A.

43 J. N. Israelachvili, *Intermolecular and Surface Forces*, Academic Press, Burlington (Mass.), 3rd edn, 2011.

44 J. Gao, W. D. Luedtke, D. Gourdon, M. Ruths, J. N. Israelachvili and U. Landman, Frictional Forces and Amontons' Law: From the Molecular to the Macroscopic Scale, *J. Phys. Chem. B*, 2004, **108**(11), 3410–3425, DOI: 10.1021/jp036362l.

45 R. S. Johansson and A. B. Vallbo, Tactile Sensibility in the Human Hand: Relative and Absolute Densities of Four Types of Mechanoreceptive Units in Glabrous Skin, *J. Physiol.*, 1979, **286**(1), 283–300, DOI: 10.1113/jphysiol.1979.sp012619.

46 P. W. Nye and J. C. Bliss, Sensory Aids for the Blind: A Challenging Problem with Lessons for the Future, *Proc. IEEE*, 1970, **58**(12), 1878–1898.

47 P. L. Ray, A. P. Cox, M. Jensen, T. Allen, W. Duncan and A. D. Diehl, Representing Vision and Blindness, *J. Biomed. Semant.*, 2016, **7**(1), 15, DOI: 10.1186/s13326-016-0058-0.

48 L. M. Schriml, J. B. Munro, M. Schor, D. Olley, C. McCracken, V. Felix, J. A. Baron, R. Jackson, S. M. Bello, C. Bearer, R. Lichenstein, K. Bisordi, N. C. Dialo, M. Giglio and C. Greene, The Human Disease Ontology 2022 Update, *Nucleic Acids Res.*, 2022, **50**(D1), D1255–D1261, DOI: 10.1093/nar/gkab1063.

49 D. N. Saito, T. Okada, M. Honda, Y. Yonekura and N. Sadato, Practice Makes Perfect: The Neural Substrates of Tactile Discrimination by Mah-Jong Experts Include the Primary Visual Cortex, *BMC Neurosci.*, 2006, **7**(1), 79, DOI: 10.1186/1471-2202-7-79.

50 A. Bubic, E. Striem-Amit and A. Amedi, Large-Scale Brain Plasticity Following Blindness and the Use of Sensory Substitution Devices. in *Multisensory Object Perception in the Primate Brain*, ed. J. Kaiser and M. J. Naumer, Springer New York, New York, NY, 2010, pp. 351–380, DOI: 10.1007/978-1-4419-5615-6_18.

51 N. Sadato, T. Okada, M. Honda and Y. Yonekura, Critical Period for Cross-Modal Plasticity in Blind Humans: A Functional MRI Study, *NeuroImage*, 2002, **16**(2), 389–400, DOI: 10.1006/nimg.2002.1111.

52 H. Burton, R. J. Sinclair and D. G. McLaren, Cortical Activity to Vibrotactile Stimulation: An fMRI Study in Blind and Sighted Individuals, *Hum. Brain Mapp.*, 2004, **23**(4), 210–228, DOI: 10.1002/hbm.20064.

53 A. Bhattacharjee, A. J. Ye, J. A. Lisak, M. G. Vargas and D. Goldreich, Vibrotactile Masking Experiments Reveal Accelerated Somatosensory Processing in Congenitally Blind Braille Readers, *J. Neurosci.*, 2010, **30**(43), 14288–14298, DOI: 10.1523/JNEUROSCI.1447-10.2010.

54 Z. Cattaneo and T. Vecchi, *Blind Vision: The Neuroscience of Visual Impairment*, MIT press, 2011.

55 L. Gao and T. J. McCarthy, Contact Angle Hysteresis Explained, *Langmuir*, 2006, **22**(14), 6234–6237, DOI: 10.1021/la060254j.

56 G. Jakša, B. Štefane and J. Kovač, XPS and AFM Characterization of Aminosilanes with Different Numbers of Bonding Sites on a Silicon Wafer, *Surf. Interface Anal.*, 2013, **45**(11–12), 1709–1713, DOI: 10.1002/sia.5311.

57 R. Kesarwani, P. P. Dey and A. Khare, Correlation between Surface Scaling Behavior and Surface Plasmon Resonance Properties of Semitransparent Nanostructured Cu Thin Films Deposited *via* PLD, *RSC Adv.*, 2019, **9**(14), 7967–7974, DOI: 10.1039/C9RA00194H.

58 Y. Gong, S. T. Misture, P. Gao and N. P. Mellott, Surface Roughness Measurements Using Power Spectrum Density Analysis with Enhanced Spatial Correlation Length, *J. Phys. Chem. C*, 2016, **120**(39), 22358–22364, DOI: 10.1021/acs.jpcc.6b06635.

59 C. Yuan, Y. Yao, B. Cheng, Y. Cheng, Y. Li, Y. Li, X. Liu, X. Cheng, X. Xie and J. Wu, The Application of Deep Learning Based Diagnostic System to Cervical Squamous Intraepithelial Lesions Recognition in Colposcopy Images, *Sci. Rep.*, 2020, **10**(1), 11639.

60 F. M. Mwema, O. P. Oladijo, T. S. Sathiaraj and E. T. Akinlabi, Atomic Force Microscopy Analysis of Surface Topography of Pure Thin Aluminum Films, *Mater. Res. Express*, 2018, **5**(4), 046416.

61 C. J. Powell, Elemental Binding Energies for X-Ray Photoelectron Spectroscopy, *Appl. Surf. Sci.*, 1995, **89**(2), 141–149.

62 N. Kumar, N. K. Bhardwaj and S. K. Chakrabarti, Influence of Particle Size Distribution of Calcium Carbonate Pigments on Coated Paper Whiteness, *J. Coat. Technol. Res.*, 2011, **8**(5), 613–618, DOI: 10.1007/s11998-011-9353-y.

63 V. K. Rastogi, C. Singh, V. Jain and M. A. Palafox, FTIR and FT-Raman Spectra of 5-Methyluracil (Thymine), *J. Raman Spectrosc.*, 2000, **31**(11), 1005–1012, DOI: 10.1002/1097-4555(200011)31:11<1005::AID-JRS636>3.0.CO;2-7.

64 Y.-J. Liu, N. M. Navasero and H.-Z. Yu, Structure and Reactivity of Mixed ω-Carboxyalkyl/Alkyl Monolayers on Silicon: ATR-FTIR Spectroscopy and Contact Angle Titration, *Langmuir*, 2004, **20**(10), 4039–4050, DOI: 10.1021/la035813q.

65 H. A. Al-Abadleh and V. H. Grassian, FT-IR Study of Water Adsorption on Aluminum Oxide Surfaces, *Langmuir*, 2003, **19**(2), 341–347, DOI: 10.1021/la026208a.

66 M. Wang, K. M. Liechti, Q. Wang and J. M. White, Self-Assembled Silane Monolayers: Fabrication with Nanoscale Uniformity, *Langmuir*, 2005, **21**(5), 1848–1857, DOI: 10.1021/la048483y.

67 K. Viswanathan, N. K. Sundaram and S. Chandrasekar, Stick-Slip at Soft Adhesive Interfaces Mediated by Slow Frictional Waves, *Soft Matter*, 2016, **12**(24), 5265–5275.

68 B. N. J. Persson, O. Albohr, C. Creton and V. Peveri, Contact Area between a Viscoelastic Solid and a Hard, Randomly Rough, Substrate, *J. Chem. Phys.*, 2004, **120**(18), 8779–8793.

69 R. S. Johansson and J. R. Flanagan, Coding and Use of Tactile Signals from the Fingertips in Object Manipulation Tasks, *Nat. Rev. Neurosci.*, 2009, **10**(5), 345–359.

70 M. Janko, R. Primerano and Y. Visell, On Frictional Forces between the Finger and a Textured Surface during Active Touch, *IEEE Trans. Haptics*, 2015, **9**(2), 221–232.

71 D. Gueorguiev, S. Bochereau, A. Mouraux, V. Hayward and J.-L. Thonnard, Touch Uses Frictional Cues to Discriminate Flat Materials, *Sci. Rep.*, 2016, **6**(1), 25553.

72 J. Lo and R. S. Johansson, Regional Differences and Inter-individual Variability in Sensitivity to Vibration in the Glabrous Skin of the Human Hand, *Brain Res.*, 1984, **301**(1), 65–72.

73 A. Handler and D. D. Ginty, The Mechanosensory Neurons of Touch and Their Mechanisms of Activation, *Nat. Rev. Neurosci.*, 2021, **22**(9), 521–537.

74 R. Fagiani, F. Massi, E. Chatelet, Y. Berthier and A. Sestieri, Experimental Analysis of Friction-Induced Vibrations at the Finger Contact Surface, *Proc. Inst. Mech. Eng., Part J*, 2010, **224**(9), 1027–1035, DOI: 10.1243/13506501JET722.

75 L. B. Baker and A. S. Wolfe, Physiological Mechanisms Determining Eccrine Sweat Composition, *Eur. J. Appl. Physiol.*, 2020, **120**(4), 719–752, DOI: 10.1007/s00421-020-04323-7.

76 M. Brió Pérez, M. Cirelli and S. De Beer, Degrafting of Polymer Brushes by Exposure to Humid Air, *ACS Appl. Polym. Mater.*, 2020, **2**(8), 3039–3043, DOI: 10.1021/acsapm.0c00474.

77 X. Chen, S. Chen, Y. Zhang and H. Yang, Study on Functionality and Surface Modification of a Stair-Step Liquid-Triggered Valve for On-Chip Flow Control, *Micromachines*, 2020, **11**(7), 690.

78 E. Asenath Smith and W. Chen, How To Prevent the Loss of Surface Functionality Derived from Aminosilanes, *Langmuir*, 2008, **24**(21), 12405–12409, DOI: 10.1021/la802234x.